Population specific template construction and brain structure segmentation using deep learning methods

Raghav Mehta

Human Brain

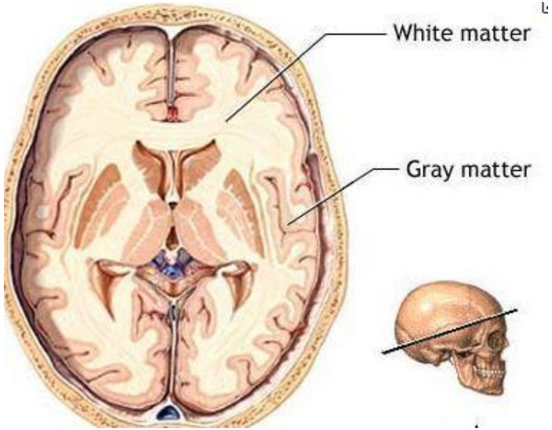

WM and GM in Human brain

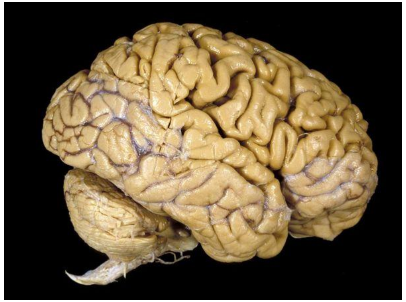

Human Brain

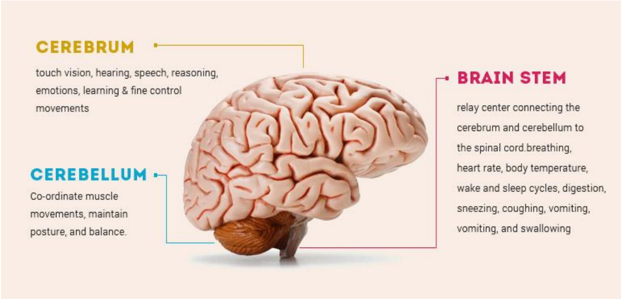

Cerebrum, Brainstem and Cerebellum

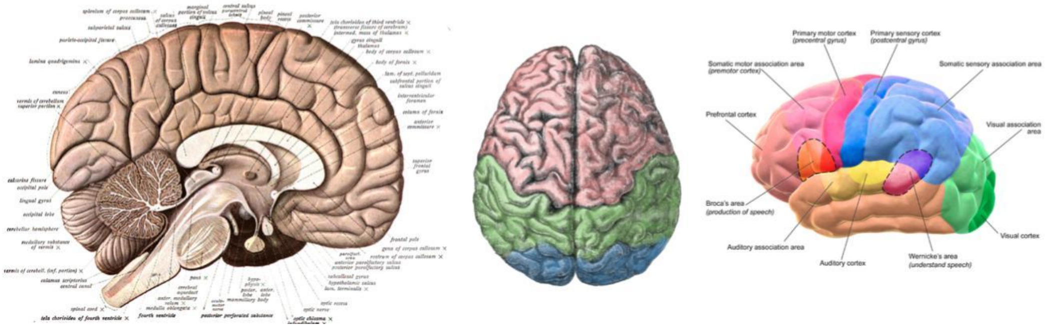

Structural (A) and Functional (B and C) areas of the human brain.

NeuroImaging Modalities

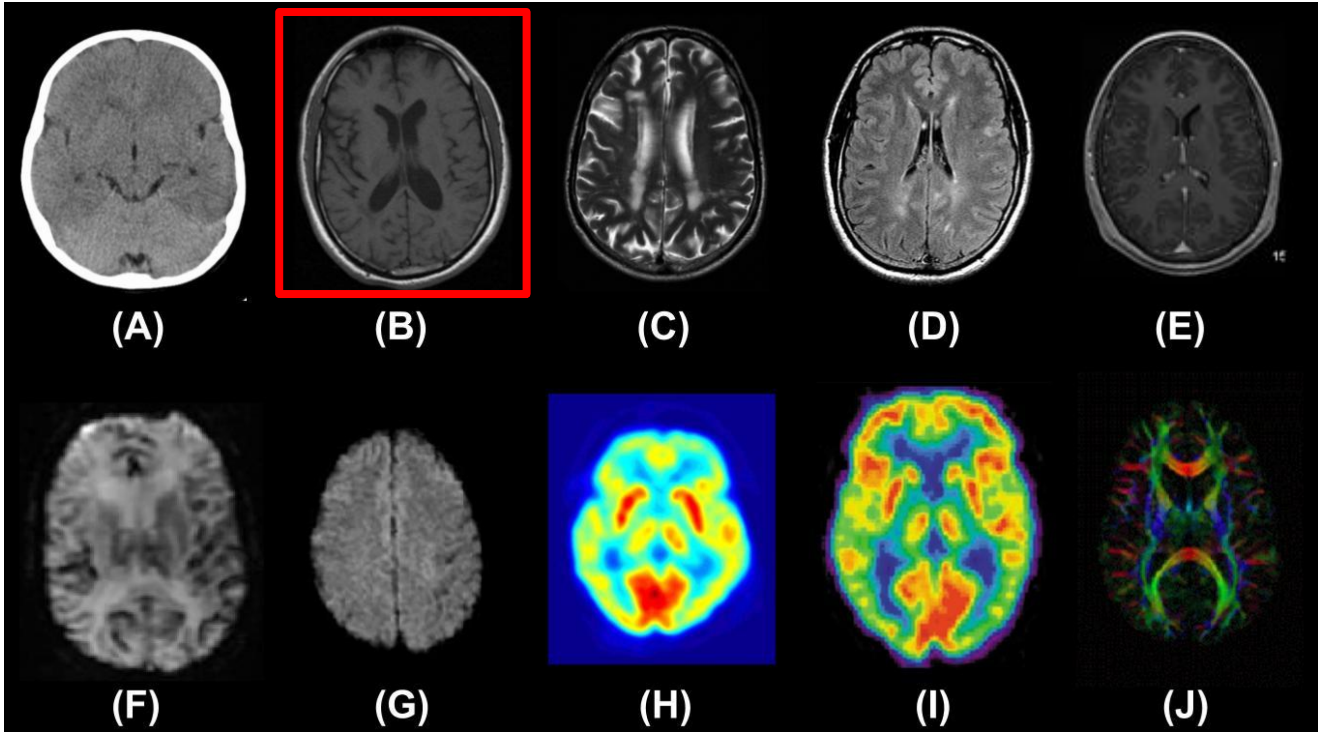

(A) CT (B) T1 (C) T2 (D) FLAIR (E) T1 with contrast (F) PWI (G) DWI (H) SPECT (I) PET (J) DTI

Thesis Focus

- Human Brain Atlas

The human brain atlas represents a distinct anatomical portrayal of the brain depicting finer anatomical details. This atlas provides a standard framework in which population based assessment of brain function and anatomy is possible.

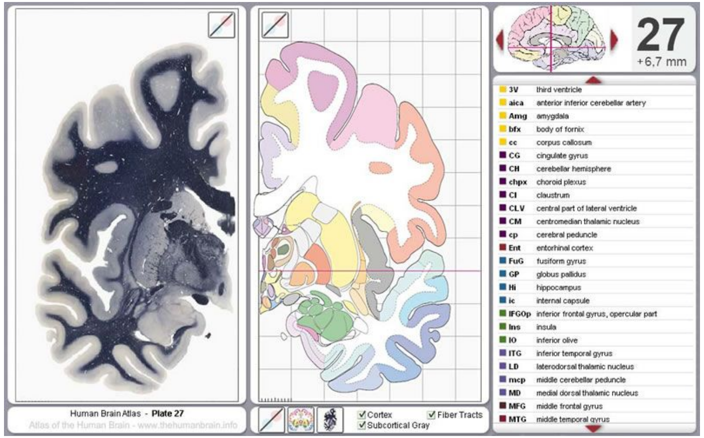

Coronal section of brain with structure segmentation

Image courtesy:
http://www.thehumanbrain.info/

Atlas ?

World

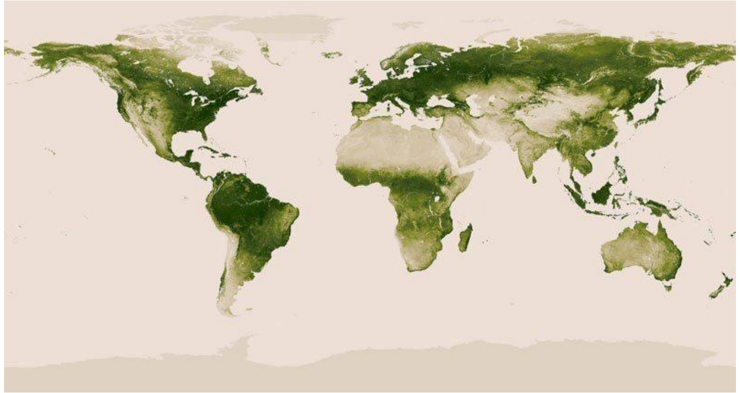

Vegetation on earth
NASA/NOAA

World Demography

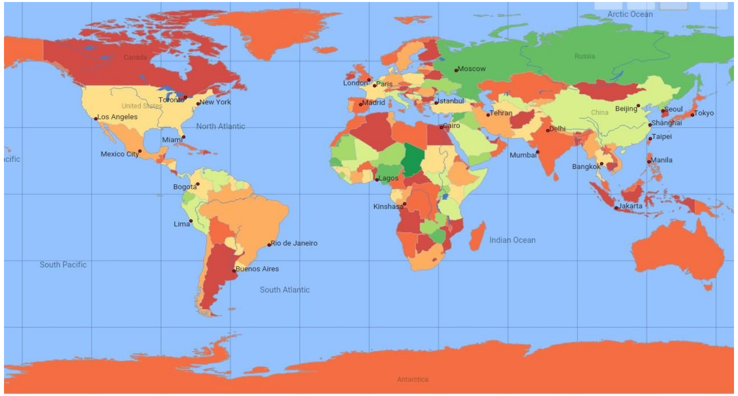

Human brain atlas

Brain atlas examples: brain template, structural atlas, functional atlas, tractography atlas, probabilistic activity map etc.

We will focus on the following two:

1. Population specific brain template
2. Structural atlas

MNI template

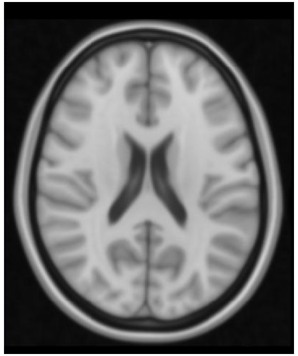

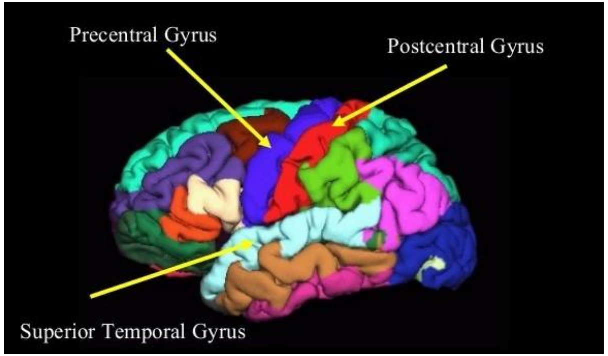

DK atlas

Thesis Overview

1. Population specific template construction for young Indian population

2. Brain structural segmentation using Deep Learning methods

   a. Patch - based approach for whole brain segmentation

   b. Fully convolutional approach for sub-cortical segmentation

Thesis Overview

1. **Population specific template construction for young Indian population**

2. Brain structural segmentation using Deep Learning methods

   a. Patch - based approach for whole brain segmentation

   b. Fully convolutional approach for sub-cortical segmentation

Need for population specific template

- The significant difference in the shape and the size of human brains across different races pose a great challenge for functional and structural comparison analysis in neuroscience research
- Popular MNI152 [3] template is based on MRIs of the caucasian population.
- Recent studies have shown morphological difference between brain MRI of the caucasian and the eastern population [4,5,6,7].
- Some recent templates:
    - Chinese56 [4]
    - Chinese2020 [5]
    - Korean78 [6]
    - Korean96 [7]
    - French [8]
    - Colin27 [9]

Dataset

- 100 Young Adult, Age: 21 - 30 years (50M/50F)
- 1.5T T1 MRI
  - Voxel size: 1mm x 1mm x 1mm
  - Acquisition matrix: 256 x 256
  - Sagittal slices: 192

- **Siemens**
  - MPRAGE
  - TR: 2370 ms
  - TE: 2.9 ms
  - TI: 1000 ms
  - Flip angle: 7°
- **GE**
  - BRAVO
  - TR: 10.2 ms
  - TE: 4.2 ms
  - TI: 450 ms
  - Flip angle: 15°
- **Phillips**
  - 3D TFE SENSE
  - TR: 8.2 ms
  - TE: 3.8 ms
  - TI: -
  - Flip angle: 7°

Age Distribution

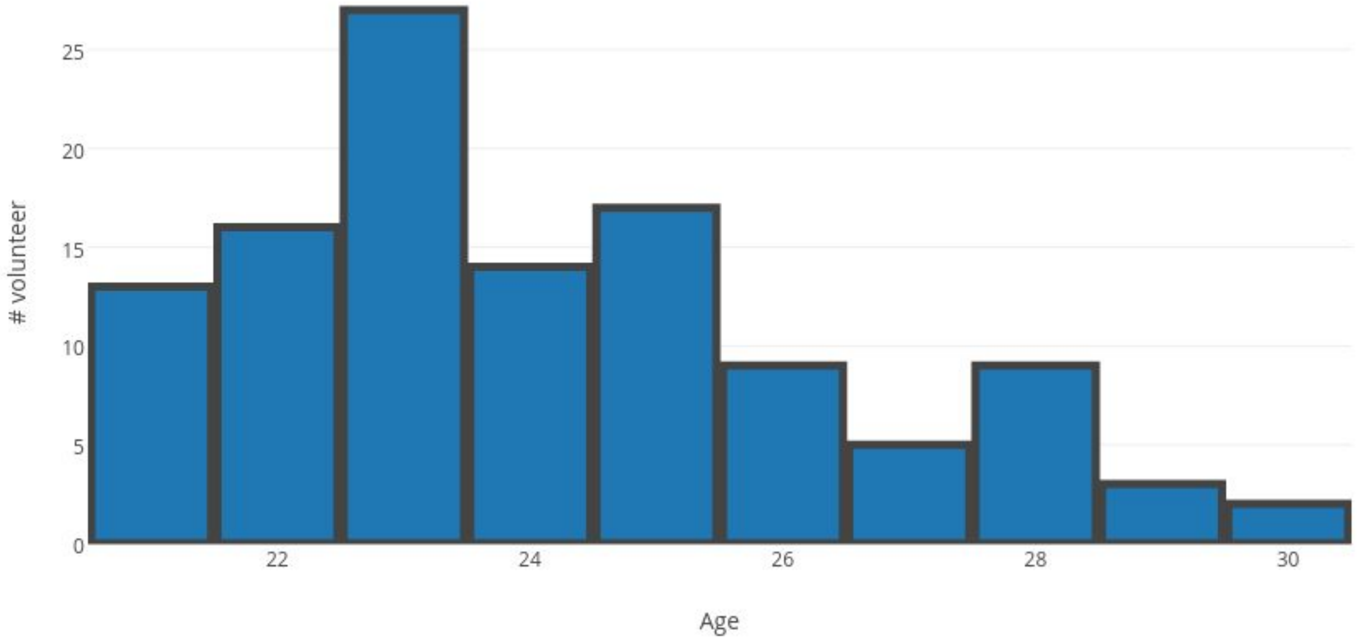

Data Pre-processing

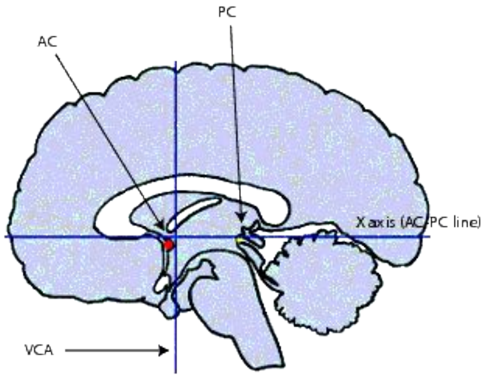

1. AC-PC alignment [10]
2. N4-bias field correction [11]
3. Non Local Mean based denoising [12]
4. Skull - stripping using BET [13]
5. Intensity standardization [14]

Template Construction

- Use of ANTs tool*
- Groupwise Registration Based on "The optimal template effect in hippocampus studies of diseased populations." Avants et al. [15]
  - Multiscale Method
  - Symmetric Registration
  - Appearance and Shape guided Registration

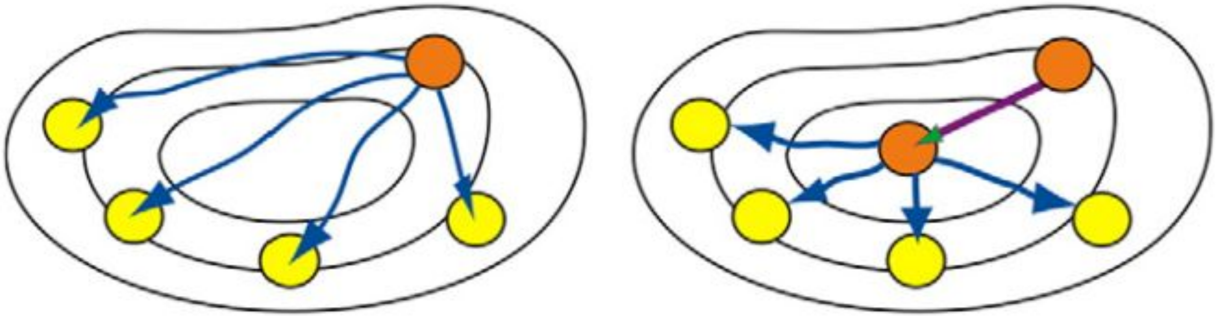

* stnava.github.io/ANTs/

Indian Brain Template

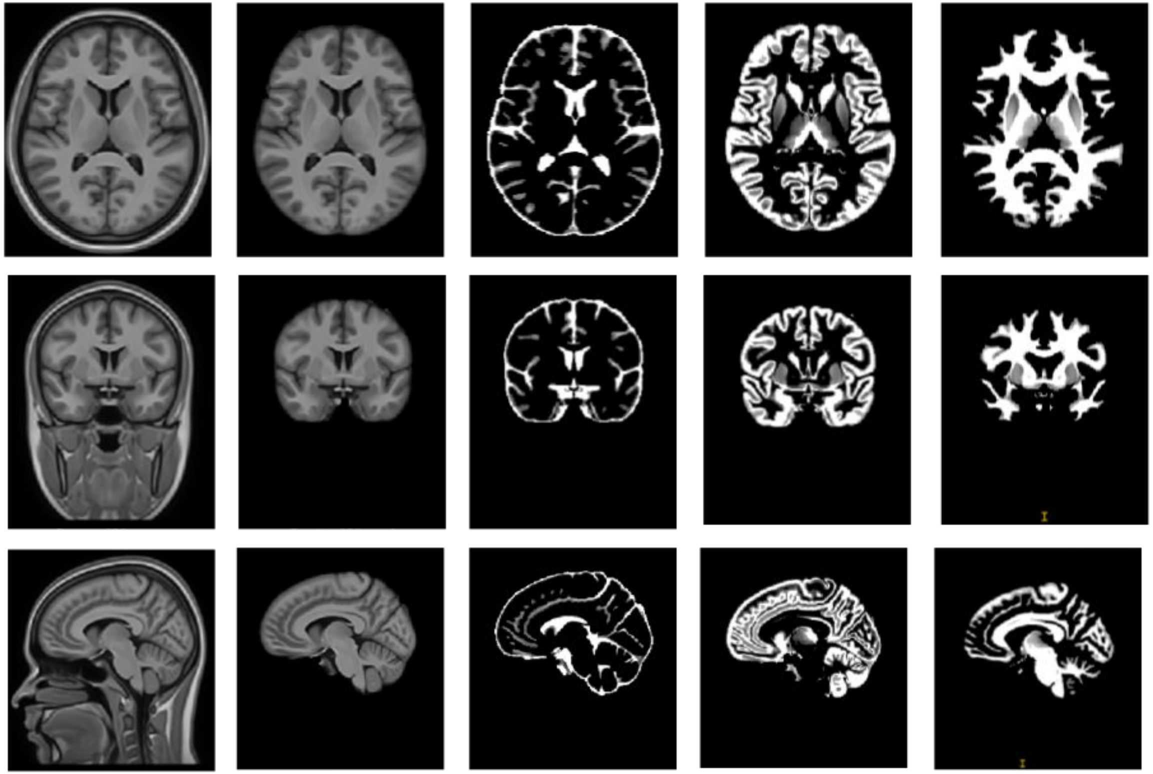

Axial

Coronal

Sagittal

MRI volume | Brain | CSF | GM | WM

Indian Brain Template

Axial

Coronal

Sagittal

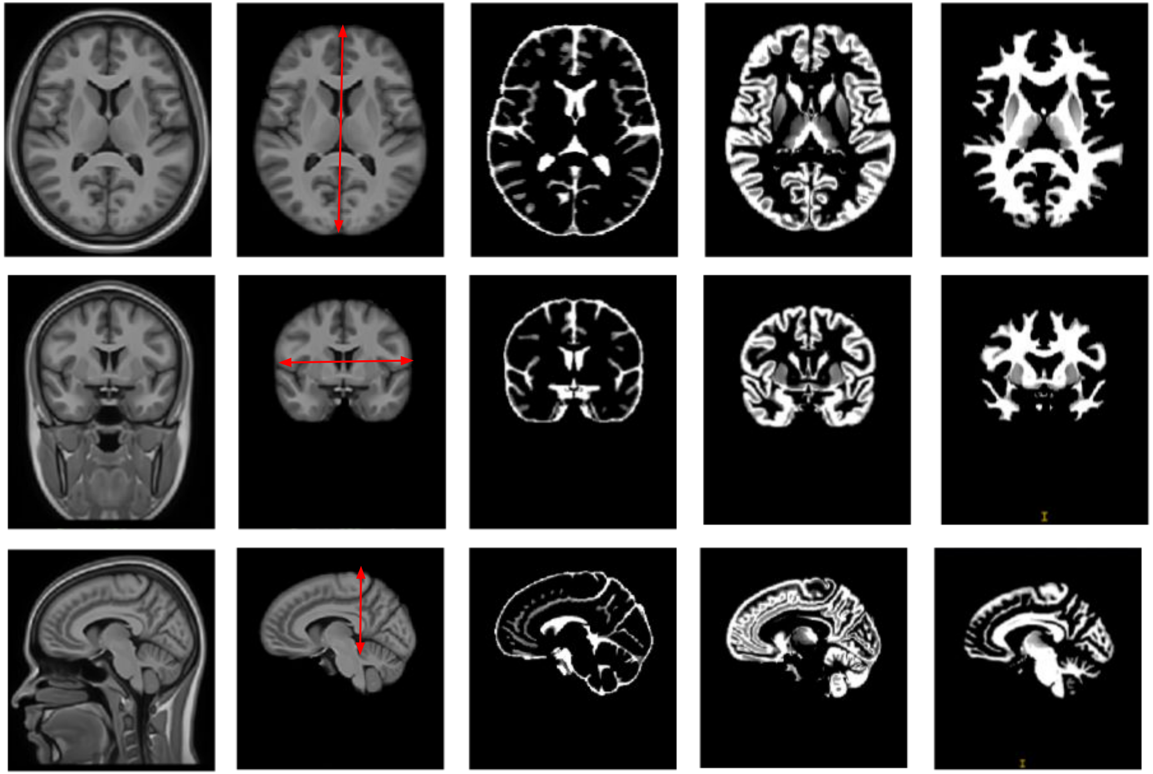

MRI volume | Brain | CSF | GM | WM

Comparison with different template

	AC-PC (mm)	Length (mm)	Width (mm)	Heigth (mm)	W/L	H/L	H/W	Volume (dm^3)
IBA100	25	160	130	88	0.81	0.55	0.68	1.39
IBA50M	25	162	131	91	0.81	0.56	0.69	1.45
IBA50F	24	157	128	86	0.82	0.55	0.67	1.32
Talairach	-	180	146	115	0.81	0.64	0.79	-
MNI152	28	179	142	110	0.79	0.61	0.77	2.06
ICBM452	28	176	144	109	0.81	0.57	0.70	1.56
Chinese56	26	175	145	100	0.83	0.57	0.69	1.89
Chinese2020	26	162	137	94	0.85	0.58	0.69	1.51
Korean96	26	160	136	92	0.85	0.58	0.68	1.63

Comparison of Brain Size and shape of Indian Templates and other templates

Need for gender specific template

	AC-PC (mm)	Length (mm)	Width (mm)	Heigth (mm)	W/L	H/L	H/W	Volume (dm^3)
Young Adults	25.27 ± 1.29	159.47 ± 7.55	130.63 ± 6.10	88.75 ± 4.35	0.82 ± 0.05	0.56 ± 0.03	0.68 ± 0.04	1.44 ± 0.14
Male	25.57 ± 1.30	162.39 ± 7.73	132.92 ± 6.23	90.29 ± 4.02	0.82 ± 0.05	0.56 ± 0.02	0.68 ± 0.03	1.52 ± 0.13
Female	24.99 ± 1.23	156.67 ± 6.24	128.43 ± 5.12	87.27 ± 4.18	0.82 ± 0.05	0.56 ± 0.03	0.68 ± 0.04	1.36 ± 0.10
p-value	0.017	< 0.001	< 0.001	0.001	0.625	0.421	1.00	< 0.001

Comparison of global brain features for Indian young adult subjects in the construction group

Validation of the constructed template

Measurement	Original brain	Registered to MNI152	Registered to Chinese2020	Registered to IBA100	p-value		
					P1	P2	P3
AC-PC	25.09 ± 1.39	28.39 ± 1.19	26.52 ± 0.71	25.83 ± 0.93	< 0.0001 *	0.1349	0.2347
Length (L)	160.93 ± 4.99	179.80 ± 1.08	168.17 ± 1.45	161.80 ± 1.26	< 0.0001 *	0.0028	0.4618
Width (W)	129.93 ± 5.43	142.73 ± 1.28	134.90 ± 2.12	129.93 ± 0.88	< 0.0001 *	< 0.0001 *	0.8301
Height (H)	88.80 ± 3.41	109.07 ± 1.53	96.77 ± 2.00	89.00 ± 1.73	< 0.0001 *	< 0.0001 *	0.8177

Intensity Standardization

- MR image do not have standard intensity range for a particular organ.
- There is inter-scanner, intra-scanner, inter-subject, intra-subject variation in intensity profile of MR images

MRI slice

Intensity profile

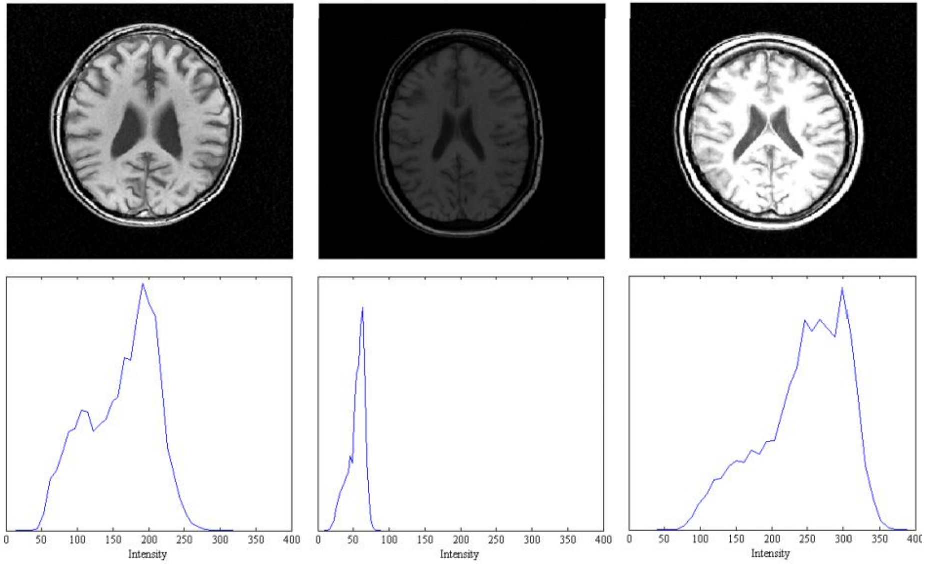

GE **Siemens** **Phillips**

Intensity Standardization

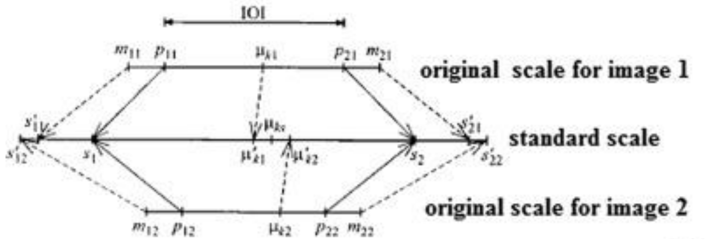

a)

Finding the parameters of the standard histogram. For illustration, only two input images are shown. For j = 1; 2, m_{1j} and m_{2j} are the minimum and maximum intensities in the image V_j , p_{1j} and p_{2j} are the minimum and maximum percentile intensities, μ_{kj} is one of the landmarks of the histogram, μ'_{kj} is the mapped value of μ_{kj} , and μ_{ks} is the mean of the μ'_{kj} ; s: the actual parameter we are looking for on the standard scale.

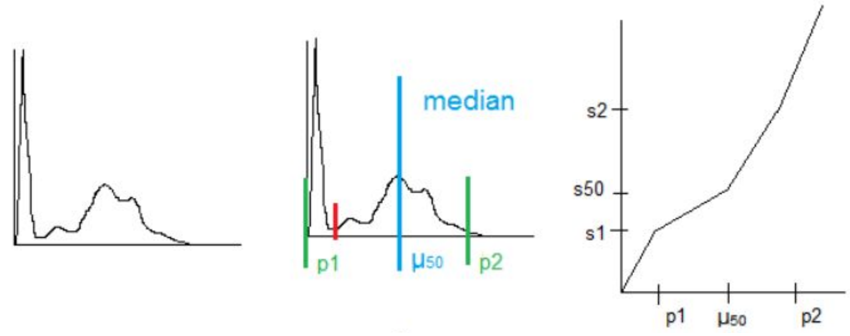

b) c) d)

b) Compute intensity histogram of scan.
c) Get the median intensity μ50, p1, and p2 as landmarks.
d) Linear piece-wise mapping to standard landmarks.

Image Courtesy: [2]

Intensity Standardization

Without tissue information [2]	Hybrid approach (proposed)	With tissue information [1]
Most Popular approach Advantages: • Based on percentiles of the global histogram • No need for tissue segmentation • Fast Disadvantage: • Tissue preservation not guaranteed	• Tissue labels required only during training • IS of a new volume does not require tissue labels • Tissue based percentiles derived from nearest pre-labelled volume • Faster than [1] • Performance is on par with [1] and superior to [2]	Recently Proposed approach Advantages: • Based on percentiles of tissue level histogram • Preserves tissue information • Better performance than [2] Disadvantage: • Needs tissue segmentation • Slow

Proposed Hybrid Approach

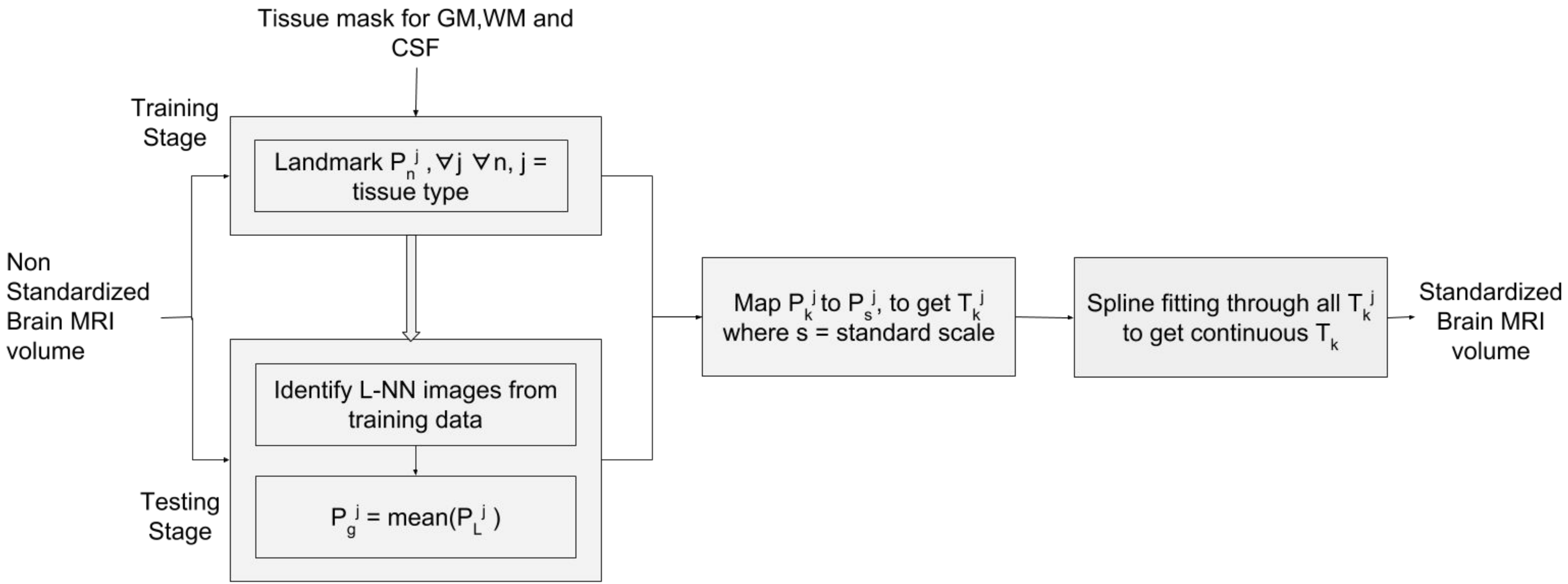

Overview of the proposed hybrid approach for intensity standardization of brain MR images

Evaluation

- 8x3 (=24) T1 weighted volumes from three different scanner manufacturers (GE, Siemens, Phillips).
- Data from scanners GE and Siemens were locally sourced; Phillips scanner data was sourced from a public dataset.

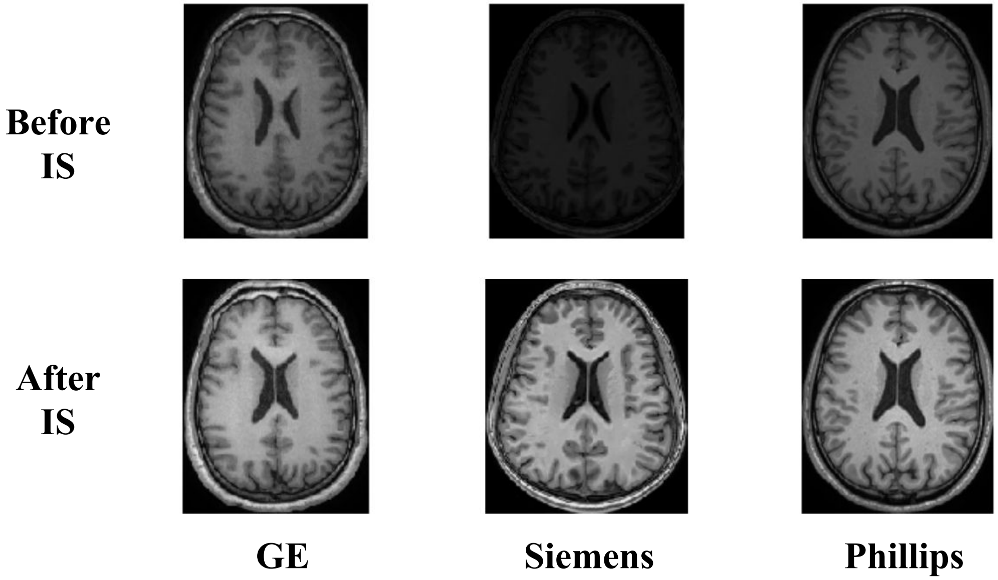

Qualitative Results (PDF)

Inter - scanner

Before IS

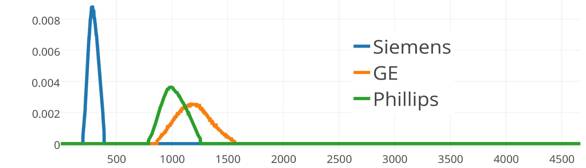

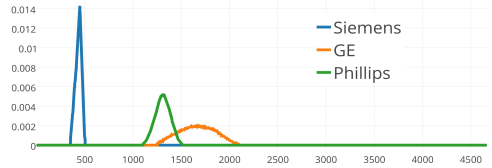

After IS

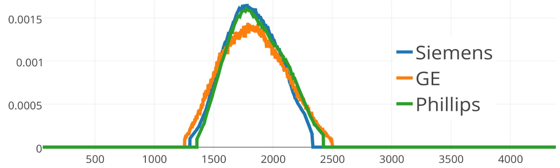

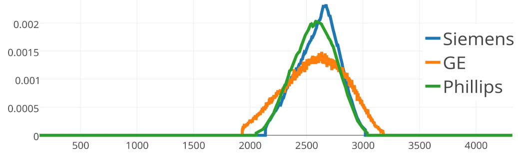

Intra - scanner

Before IS

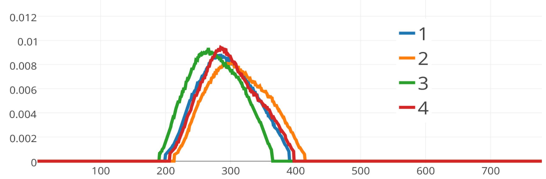

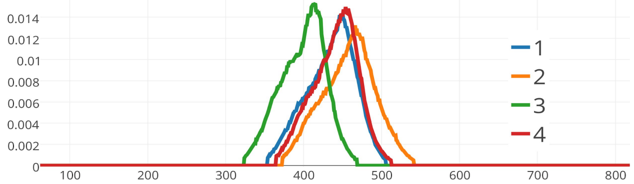

After IS

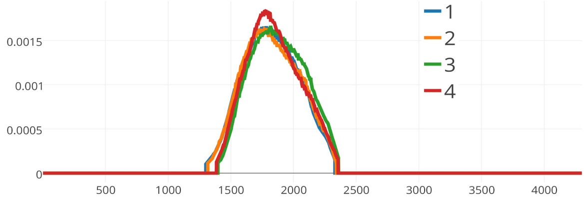

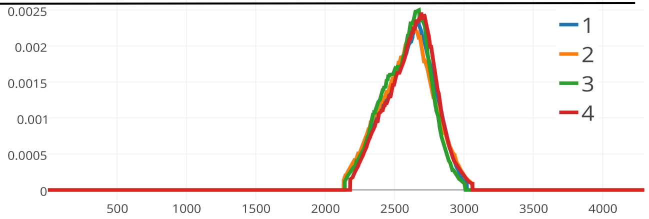

GM **WM**

Quantitative Results

$$JD_{intra}(k,j)=\frac{1}{mn}\sum_{n}\sum_{m} JD(I_n^j(k), I_m^j(k))$$
$$m\neq n, \forall n, m\in k$$

$$JD_{inter}(k_a,k_b,j)=\frac{1}{mn}\sum_{n}\sum_{m} JD(I_n^j(k_a), I_m^j(k_b))$$
$$\forall n\in k_a, \forall m\in k_b$$

		Intra-scanner JD (in x 10-2)			Inter-scanner JD			NMI statistics (across all volumes)		
		G	S	P	G vs S	G vs P	S vs P	σ_{NMI}	μ_{NMI}	% CV
CSF	Before IS	7.99	6.06	2.04	1.25	0.28	1.10	0.0240	0.1444	16.621
	[2]	3.87	2.74	0.97	0.08	0.03	0.05	0.0127	0.2228	5.7001
	ours	3.53	2.40	0.87	0.04	0.03	0.04	0.0055	0.2506	2.1942
	[1]	3.50	2.35	0.84	0.03	0.02	0.03	0.0049	0.2412	2.0315
GM	Before IS	16.32	9.28	3.34	1.38	0.48	1.23	0.0305	0.2676	11.399
	[2]	7.70	3.54	2.28	0.15	0.08	0.05	0.0128	0.4129	3.1001
	ours	5.78	2.32	1.35	0.04	0.05	0.03	0.0094	0.4444	2.1152
	[1]	5.67	2.28	1.32	0.03	0.03	0.02	0.0084	0.4427	1.8974
WM	Before IS	19.53	8.71	3.46	1.38	0.88	1.25	0.0285	0.4049	7.0391
	[2]	7.56	5.25	2.95	0.44	0.25	0.14	0.0196	0.5792	3.3836
	ours	5.32	2.47	2.27	0.09	0.07	0.05	0.0119	0.6200	1.9193
	[1]	5.19	2.40	2.19	0.07	0.05	0.04	0.0106	0.6205	1.7082

Thesis Overview

1. Population specific template construction for young Indian population

2. **Brain structural segmentation using Deep Learning methods**

   a. Patch - based approach for whole brain segmentation

   b. Fully convolutional approach for sub-cortical segmentation

Need for automatic structural segmentation

- Quantitative analysis of the neuroimaging data requires cortical and non-cortical structural segmentation.

- Useful for assessment of various neurodegenerative disorders, fMRI studies, connectivity analysis, etc.

- Manual labelling is unsuitable as it is slow and prone to human errors.

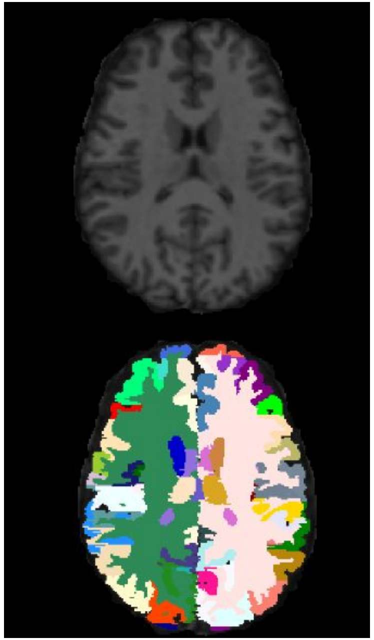

T1 MRI

Structure Segmentation

Structural segmentation

- Multi-Atlas segmentation: a popular method automatic segmentation

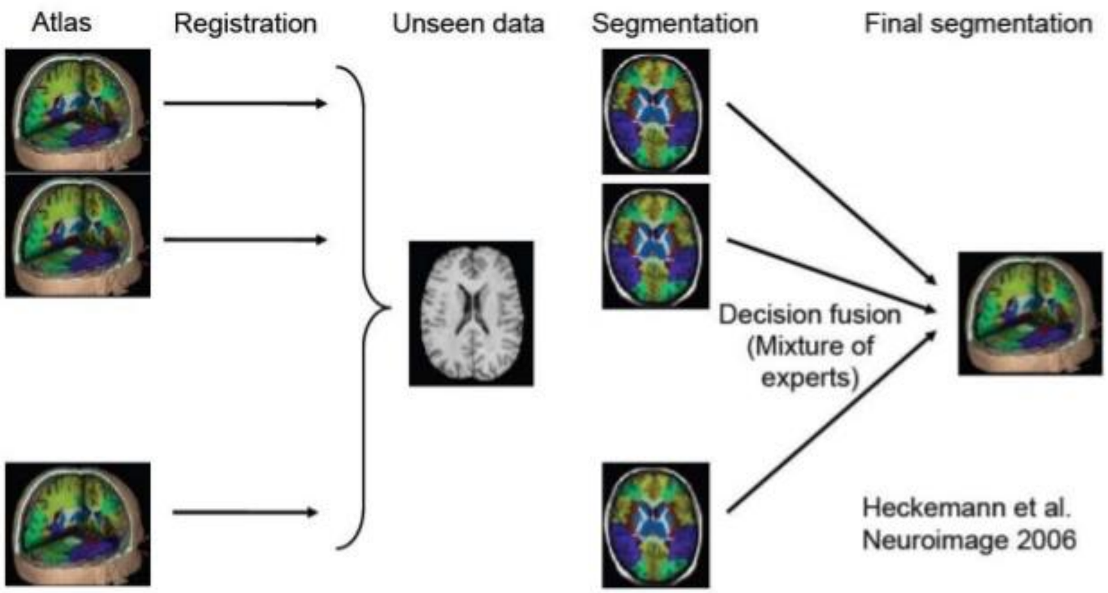

Image courtesy:
qure.ai

Literature survey

Registration based methods [16]	Patch based methods [17]
• Non-rigid registration of training atlases to a new volume • Followed by various fusion techniques • Time consuming (20-25 hours) • Not ideal for situations where segmentation in less time is required	• For a given voxel in a new volume, find similar voxels from available atlases • Segment the new volume voxel by voxel • Computational time less than the registration based approaches, but still comparatively higher (2-3 hours)

Literature survey

Model based methods [18][19]	**Machine learning based methods [20][21]**
• Learning a mathematical model based on training atlases • Segment a new volume using the learnt model • Computationally efficient (15-20 minutes)	• Learn either CNN or RF based classifier from training dataset • Segment new volume using voxel by voxel • Computationally efficient (5-10 minutes)

Proposed method - patch based approach

- Convolutional neural network based approach for the whole brain segmentation (BrainSegNet)

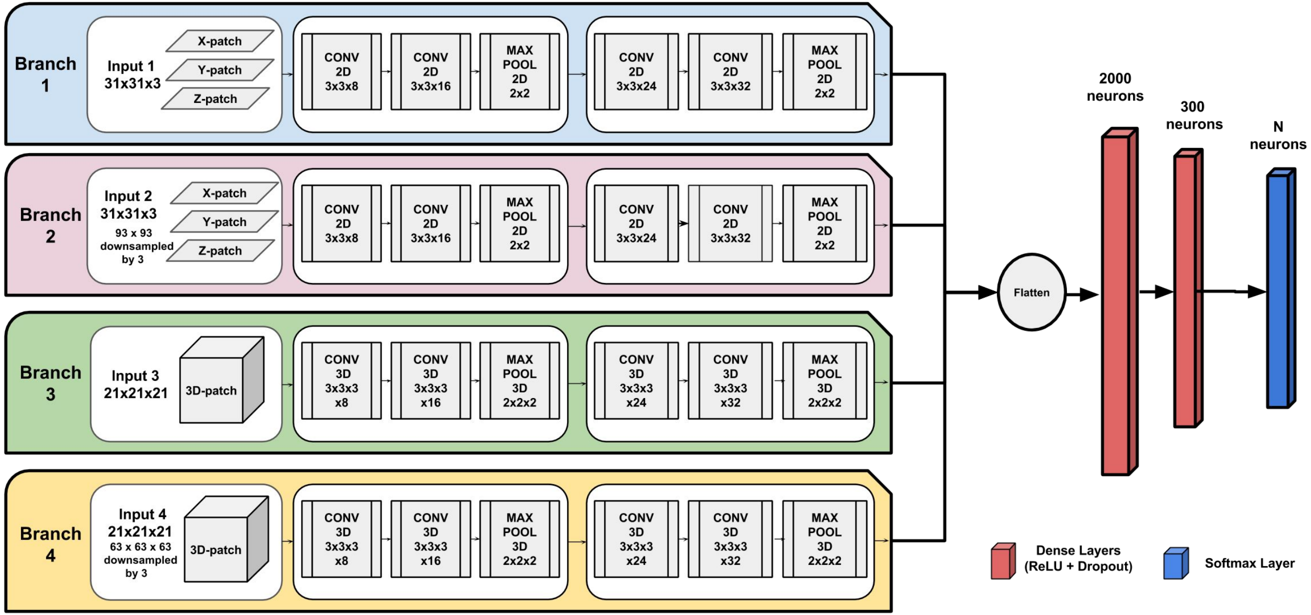

Schematic overview of the proposed CNN Architecture. The number of neurons N is same as the number of manually marked structures in a dataset (including background).

Input Patches

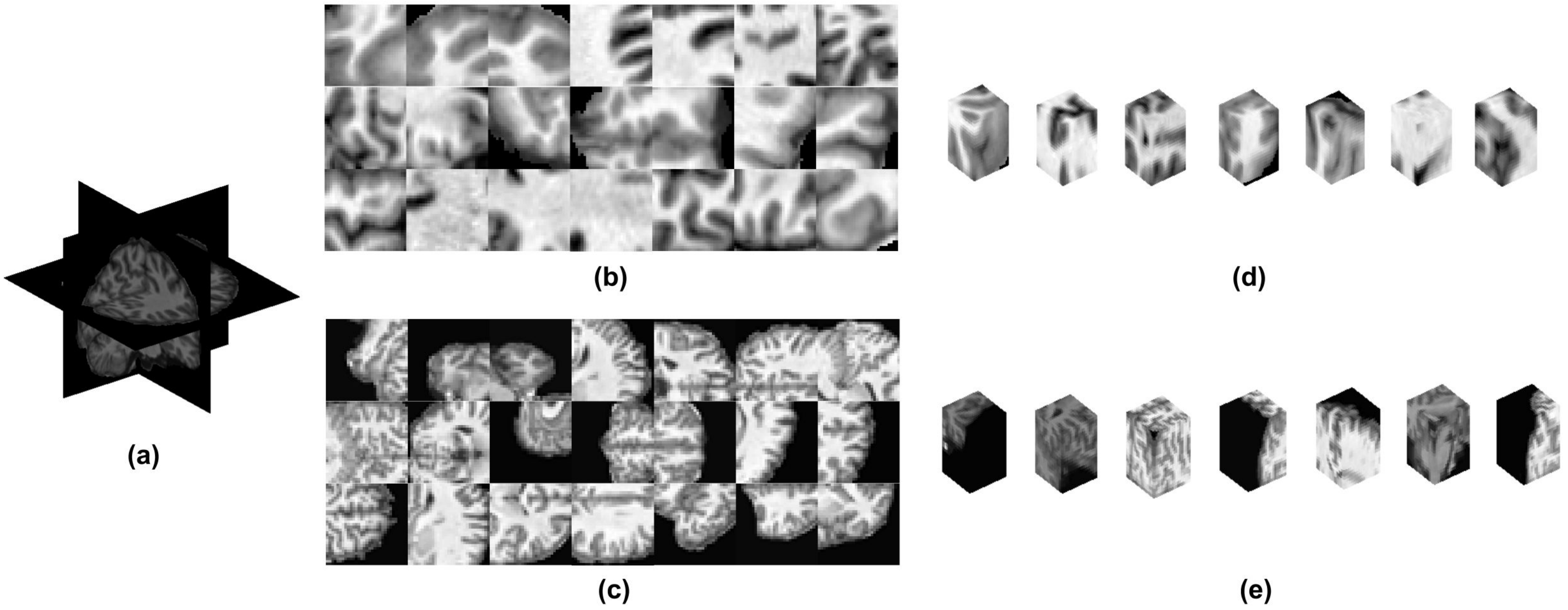

Sample input patches. (a) 2.5D representation of the brain MRI volume. For seven different voxels, the Branch 1 (31x31x3) (b), Branch 2 (93/3 x 93/3 x 3) (c), Branch 3 (21x21x21) (d) and Branch 4 (63/3 x 63/3 x 63/3) (e) patches/cubes are also shown. The ordering for (b) and (c) are: coronal (top row), sagittal (middle row) and axial (bottom row) slices.

Datasets

MRI slice

Manual Segmentation

Automatic Segmentation Using BrainSegNet

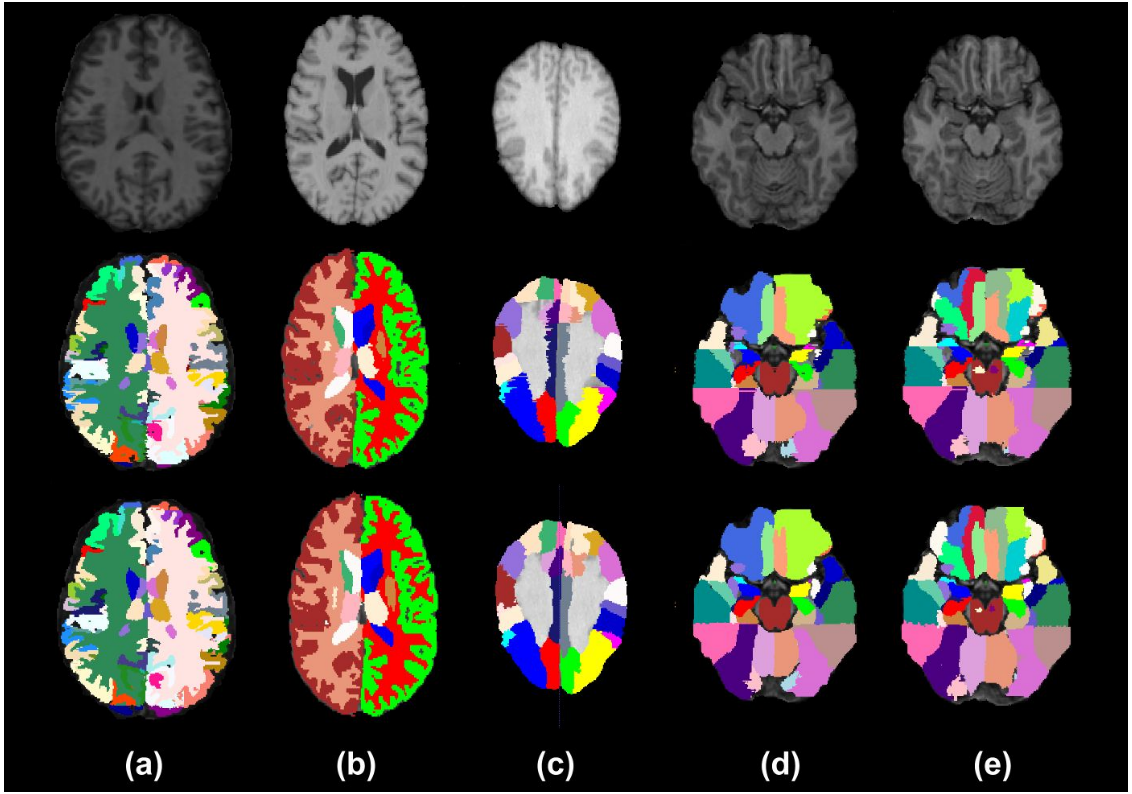

(a) MICCAI-2012 (b) IBSR (c) LONI-LPBA40 (d) Hammers67n20 (e) Hammers83n30

Qualitative Results

- Let A and B denote the binary segmentation labels generated manua and computationally, respectively. The DC is defined as: $DC(A, B) = \frac{2|AB|}{|A| + |B|}$

Dataset	Various method	State-of-the-art	BrainSegNet
MICCAI-2012[1]	0.711 - 0.764	**0.764**	0.743
IBSR[2]	0.81 - 0.835	0.835	**0.844**
LONI-LPBA40[3]	0.783 - 0.814	0.814	**0.824**
Hammers67n20[4]	0.754 - 0.836	0.836	**0.840**
Hammers83n30[4]	0.752 - 0.801	0.801	**0.808**

Performance (Mean DC) comparison of the BrainSegNet with the various methods (MALP based, patch based and classification based) for different datasets

1. https://masi.vuse.vanderbilt.edu/workshop2012
2. http://www.nitrc.org/projects/ibsr
3. http://loni.usc.edu/atlases/Atlas_Methods.php?atlas_id=12
4. http://brain-development.org/brain-atlases/

Comparison of different variants

	Cortical structures	Non-cortical structures	Overall
CNN1	0.6303±0.023	0.7701±0.024	0.6685±0.021
CNN2a	0.6370±0.011	0.7535±0.024	0.6683±0.010
CNN2b	0.6576±0.011	0.7604±0.028	0.6852±0.012
CNN3	0.6758±0.013	0.7793±0.022	0.7036±0.011
BrainSegNet	**0.7204±0.012**	**0.8053±0.028**	**0.7432±0.019**

mean DC values for different variants of the proposed CNN architecture on MICCAI-2012 dataset.

Sub-cortical segmentation

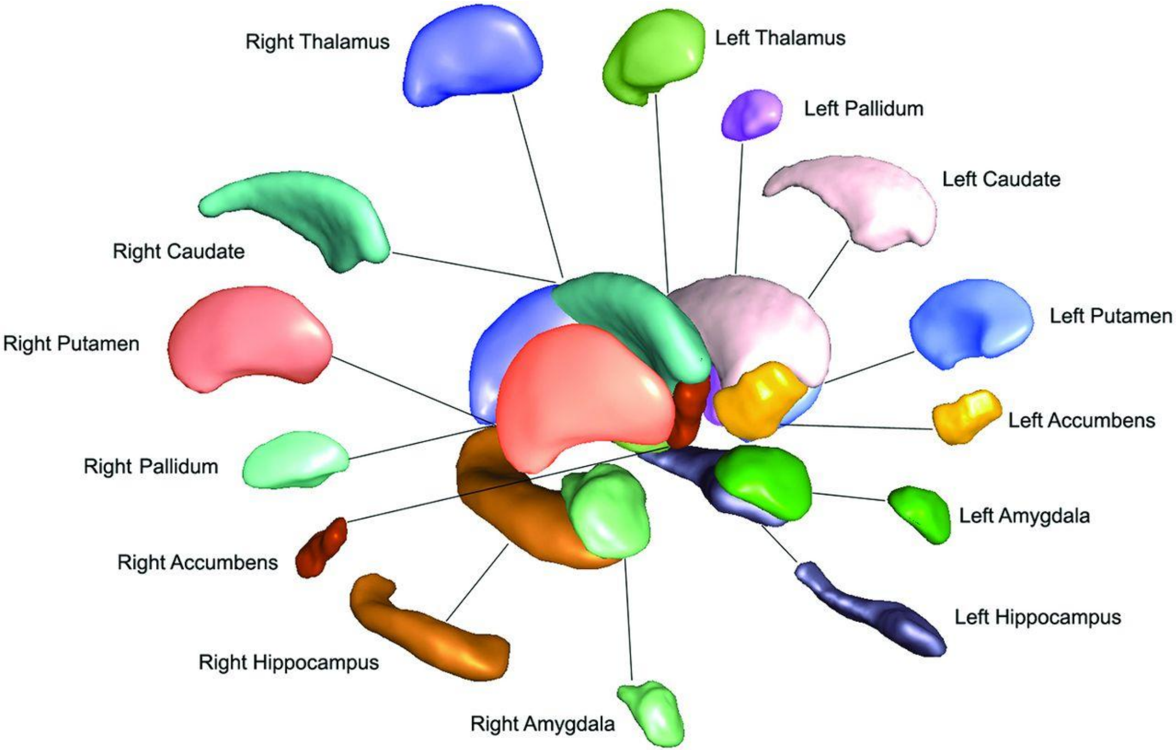

Image Courtesy: M. Walterfang, et al., “Subcortical volumetric reductions in adult niemann-pick disease type c: a cross-sectional study,” American Journal of Neuroradiology, vol. 34, no. 7, pp. 1334–1340, 2013.

Inspiration: U-net [22]

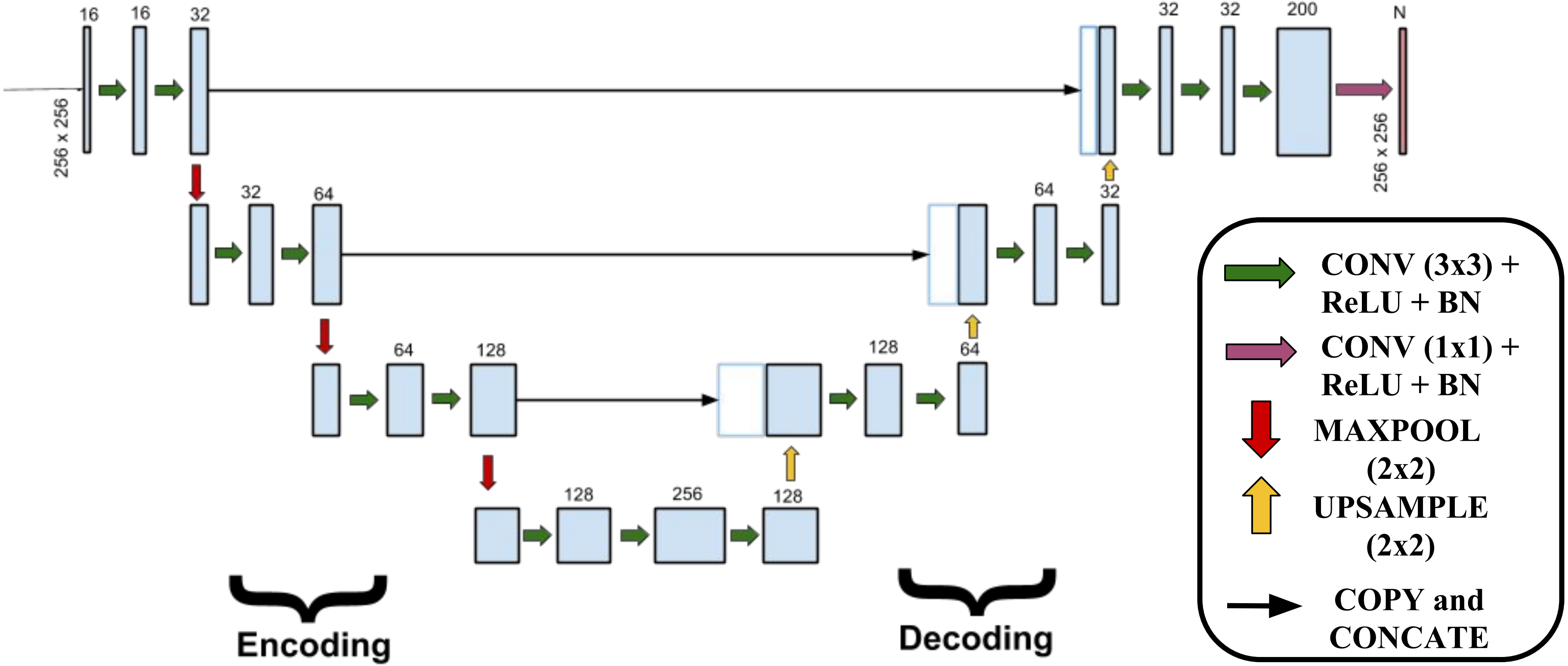

Proposed: M-net

U-net + 3D-to-2D converter + Skip Connection + Supervision

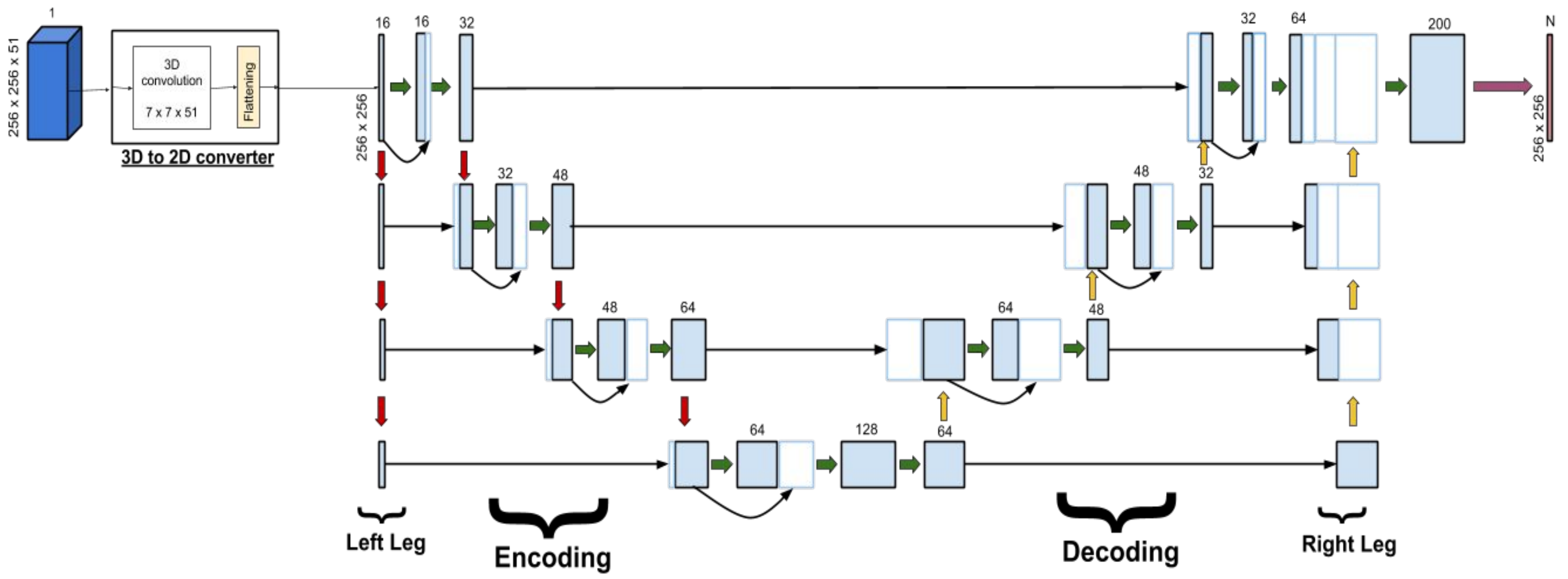

Datasets

- Two Datasets:
  - Internet Brain Segmentation Repository (IBSR)
  - MICCAI-2013 SATA Diencephalon Challenge (Mid-brain) - Free Competition

- IBSR has 18 volumes, while SATA dataset has 35 training and 12 testing volumes

- Both dataset has total 7 subcortical (left/right) structures marked; namely, Amygdala, Caudate, Putamen, Pallidum, Thalamus, Hippocampus and Accumbens Area

Evaluation on IBSR

	Freesurfer [18]	FSL [19]	RF + MRF[20]	FCN + MRF[21]	MS-CN+ MRF[22]	U-net +3D-to-2D Conv [23]	M-net
Accumbens	0.69	0.73	0.60	0.63	0.69	0.71	**0.75**
Amygdala	0.69	0.70	0.62	0.64	0.67	0.70	**0.73**
Pallidum	0.71	0.76	0.62	0.75	0.80	0.80	**0.82**
Caudate	0.82	0.83	0.78	0.78	**0.87**	0.85	**0.87**
Hippocampus	0.77	0.81	0.59	0.71	**0.82**	0.81	**0.82**
Putamen	0.81	0.84	0.77	0.83	0.88	0.89	**0.90**
Thalamus	0.86	0.88	0.80	0.87	**0.90**	0.88	**0.90**
Overall	0.76	0.79	0.69	0.75	0.80	0.81	**0.83**

Mean DC comparison on IBSR dataset for 7 sub-cortical structures

Evaluation on SATA

Mean Dice Coefficient

a) Freesurfer : 0.75761
b) FSL-FIRST : 0.82437
c) M-net : 0.85780
d) Atlas-Forest : 0.82819

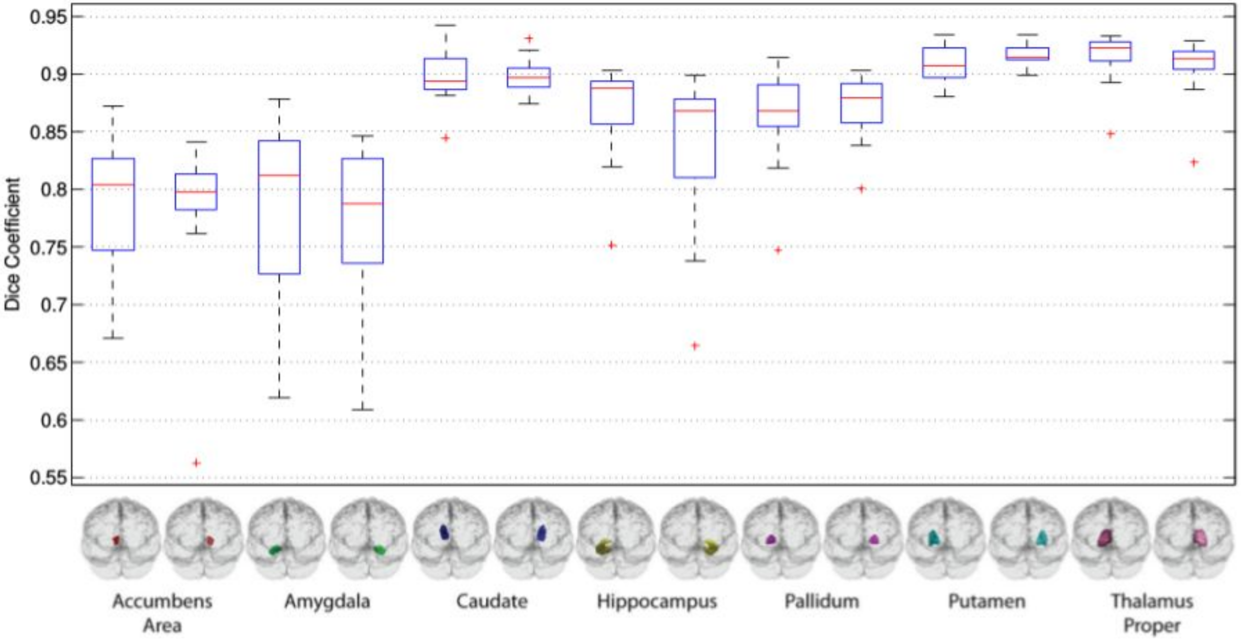

M-net: whole brain segmentation

MICCAI 2012 Multi-Atlas Labeling Challenge

- 15 Training Volumes, 20 Testing Volumes
- Segmentation into 134 structures
  - 98 cortical
  - 36 non-cortical

Mean Dice Coefficient

(1)	U-net 2D	:	0.6624
(2)	U-net + 3D-to-2D conv	:	0.6971
(3)	M-net	:	0.7278
(4)	BrainSegNet	:	0.7430
(5)	MAS (state-of-the-art)	:	**0.7640**

References

1. Nyul et al., “New variants of a method of mri scale standardization,” IEEE TMI, vol. 19, no. 2, pp.143–150, (2000).
2. Giorgio De Nunzio et al., “Robust intensity standardization in brain magnetic resonance images,” Journal of digital imaging, pp. 1–11, (2015).
3. J. Mazziotta, et al., “A probabilistic atlas and reference system for the human brain: International consortium for brain mapping (icbm),” Philosophical Transactions of the Royal Society of London B: Biological Sciences, vol. 356, no. 1412, pp. 1293–1322, (2001).
4. Tang, Y. et al., “The construction of a Chinese MRI brain atlas: A morphometric comparison study between Chinese and Caucasian cohorts.” Neuroimage, 51(1), pp.33-41. (2010).
5. Liang, P., et al.,.”Construction of brain atlases based on a multi-center MRI dataset of 2020 Chinese adults.” Scientific reports, 5. (2015)
6. Lee, J. S. et al. Development of Korean standard brain templates. J. Korean Med. Sci. 20, 483–488 (2005).
7. Lee, Hyunna, et al. "Construction and validation of brain MRI templates from a Korean normal elderly population." Psychiatry investigation 13, no. 1: 135-145 (2016).
8. Lalys F, et al. “Construction and assessment of a 3-T MRI brain template.” Neuroimage 49, 345-354 (2010)
9. Collins, D.L. et al., 1995. “Automatic 3‐D model‐based neuroanatomical segmentation.” Human brain mapping, 3(3), pp.190-208. (1995)
10. Ardekani, B. et al., “ Model-based automatic detection of the anterior and posterior commissures on MRI scans.” Neuroimage, 46(3), pp.677-682. (2009)
11. Tustison, N.J., et al. “N4ITK: improved N3 bias correction.” IEEE transactions on medical imaging, 29(6), pp.1310-1320. (2010)
12. J. V. Manjón, et al., “Adaptive non-local means denoising of mr images with spatially varying noise levels,” JMRI, vol. 31, no. 1, pp. 192–203, (2010).
13. Smith, Stephen M. "Fast robust automated brain extraction." Human brain mapping 17, no. 3 : 143-155 (2002).
14. Avants, B., “Insight into images. ch. nonrigid image registration,”
15. Avants, B. et al.“The optimal template effect in hippocampus studies of diseased populations. Neuroimage, 49(3), pp.2457-2466 (2010).
16. Iglesias, J. E., and Mert R.S.. "Multi-atlas segmentation of biomedical images: a survey." Medical image analysis 24, no. 1:205-219 (2015).
17. Coupé, P. et al. "Patch-based segmentation using expert priors: Application to hippocampus and ventricle segmentation." NeuroImage 54, no. 2: 940-954 (2011).
18. Fischl, B. et al. "Whole brain segmentation: automated labeling of neuroanatomical structures in the human brain." Neuron 33, no. 3 : 341-355 (2002).
19. Patenaude, B., et al.. "A Bayesian model of shape and appearance for subcortical brain segmentation." Neuroimage 56, no. 3 : 907-922 (2011).
20. Alchatzidis, S et al.. "Discrete multi atlas segmentation using agreement constraints." In BMVC. (2014).
21. Shakeri, M, et al.. "Sub-cortical brain structure segmentation using F-CNN's." In ISBI IEEE, pp. 269-272. (2016).
22. Bao, S et al.. "Multi-scale structured CNN with label consistency for brain MR image segmentation." Computer Methods in Biomechanics and Biomedical Engineering: Imaging & Visualization (2016): 1-5.
23. Ronneberger, O. et al. "U-net: Convolutional networks for biomedical image segmentation." In MICCAI pp. 234-241. Springer, (2015).
24. Shen, D. and Davatzikos, C., 2002. HAMMER: hierarchical attribute matching mechanism for elastic registration. IEEE TMI, 21(11), pp.1421-1439
25. Ou, Y., et al., 2011. DRAMMS: Deformable registration via attribute matching and mutual-saliency weighting. MedIA, 15(4), pp.622-639.
26. Heinrich, M.P., et al., 2012. MIND: Modality independent neighbourhood descriptor for multi-modal deformable registration. MedIA, 16(7), pp.1423-1435.
27. Heinrich, M.P., et al., 2013. Towards realtime multimodal fusion for image-guided interventions using self-similarities. In MICCAI (pp. 187-194).
28. Wu, G., et al., 2016. Scalable High-Performance Image Registration Framework by Unsupervised Deep Feature Representations Learning. IEEE TBME, 63(7), pp.1505-1516
29. Shakeri, M., et al., 2016. Prior-based Coregistration and Cosegmentation. In MICCAI (pp. 529-537).
30. Heinrich, M.P., et al., 2014. Non-parametric discrete registration with convex optimisation. In WBIR (pp. 51-61).

Thank You